LETTER

Reducing excessive GABA–mediated tonic inhibition promotes functional recovery after stroke

Andrew N. Clarkson[1]*†, Ben S. Huang[1,2]*, Sarah E. MacIsaac[1], Istvan Mody[1,2,3] & S. Thomas Carmichael[1]

Stroke is a leading cause of disability, but no pharmacological therapy is currently available for promoting recovery. The brain region adjacent to stroke damage—the peri-infarct zone—is critical for rehabilitation, as it shows heightened neuroplasticity, allowing sensorimotor functions to re-map from damaged areas[1–3]. Thus, understanding the neuronal properties constraining this plasticity is important for the development of new treatments. Here we show that after a stroke in mice, tonic neuronal inhibition is increased in the peri-infarct zone. This increased tonic inhibition is mediated by extrasynaptic GABA$_A$ receptors and is caused by an impairment in GABA (γ-aminobutyric acid) transporter (GAT-3/GAT-4) function. To counteract the heightened inhibition, we administered *in vivo* a benzodiazepine inverse agonist specific for α5-subunit-containing extrasynaptic GABA$_A$ receptors at a delay after stroke. This treatment produced an early and sustained recovery of motor function. Genetically lowering the number of α5- or δ-subunit-containing GABA$_A$ receptors responsible for tonic inhibition also proved beneficial for recovery after stroke, consistent with the therapeutic potential of diminishing extrasynaptic GABA$_A$ receptor function. Together, our results identify new pharmacological targets and provide the rationale for a novel strategy to promote recovery after stroke and possibly other brain injuries.

Stroke is a major source of disability, confining one-third of stroke survivors to nursing homes or institutional settings[4]. Recent studies have shown that the brain has a limited capacity for repair after stroke. Neural repair after stroke involves re-mapping of cognitive functions in tissue adjacent to or connected with the stroke[5,6]. Functional recovery in this peri-infarct tissue involves changes in neuronal excitability that alter the brain's representation of motor and sensory functions. Stimulation of peri-infarct cortex enhances local neuronal excitability through a process that involves long-term potentiation, alters sensorimotor maps and improves the use of affected limbs[5–8]. The inhibitory neurotransmitter GABA is critical for cortical plasticity and sensory mapping. Altering GABAergic transmission changes sensory maps during the critical period of cortical development[9] and produces rapid alterations in adult cortical maps that resemble changes occurring after stroke[10,11]. Alterations in cortical maps through blockade of GABAergic signalling are associated with fundamental changes in cellular excitability including long-term potentiation[12]. In a similar manner to normal cortical plasticity, GABAergic mechanisms may mediate changes in neuronal excitability that have a central role in functional recovery of peri-infarct cortex after stroke.

Cortical GABAergic signalling through GABA$_A$ receptors is divided into synaptic (phasic) and extrasynaptic (tonic) components. Tonically active extrasynaptic GABA$_A$ receptors set an excitability threshold for neurons[13,14]. Extrasynaptic GABA$_A$ receptors primarily consist of α5- or δ-subunit-containing receptors[13,14]. Pharmacological and genetic knockdown of α5-GABA$_A$ receptors enhance long-term potentiation and improve performance on learning and memory tasks[15,16].

The selective effects of extrasynaptic GABA$_A$ receptors on cellular excitability and plasticity, and the evidence that changes in neuronal excitability underlie functional reorganization in peri-infarct cortex, indicate that this system may have a role in recovery after stroke. We find that stroke increases tonic GABAergic transmission in peri-infarct cortex and that dampening this tonic inhibition produces an early and robust gain of motor recovery after stroke (Supplementary Fig. 1, schematic summary).

We examined neuronal excitability in the peri-infarct cortex of mice during the period of recovery and reorganization after a photothrombotic stroke to forelimb motor cortex. Whole-cell voltage-clamp recordings in *in vitro* brain slices prepared at 3, 7 and 14 days after stroke (Fig. 1a) showed a significant increase in GABA$_A$-receptor-mediated tonic inhibition (I_{tonic}) in layer 2/3 pyramidal neurons, compared to neurons from sham controls (control: 8.05 ± 0.80 pA pF^{-1}, $n = 24$, versus after stroke: 13.6 ± 1.41 pA pF^{-1}, $n = 45$, Mann–Whitney U-test, $P < 0.05$; Fig. 1b–d). I_{tonic} remained raised from 3 to 14 days after stroke (Supplementary Fig. 2a). The mean phasic excitation remained unchanged over the 2-week period after stroke
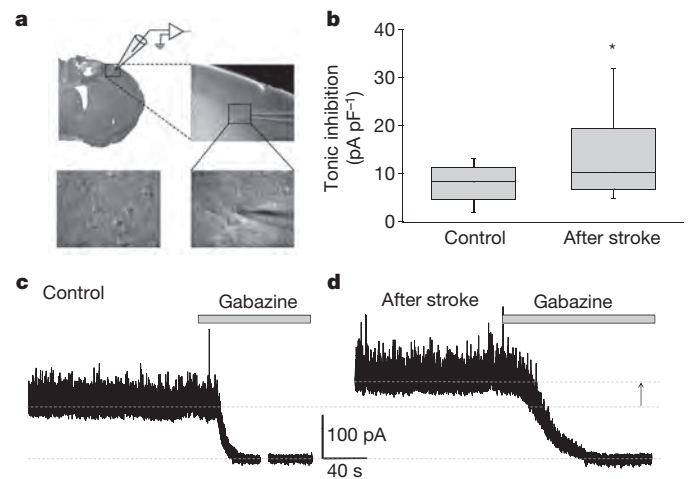

Figure 1 | Increased tonic inhibition in peri-infarct cortex. a, Images showing the peri-infarct recording site. Whole-cell patch-clamp recordings were made from post-stroke brain slices, within 200 μm of the infarct (top left; image under 2× magnification), from layer-2/3 (top right; 10×) pyramidal neurons (bottom panels; 40×). **b**, Box plot (boxes, 25–75%; whiskers, 10–90%; lines, median) showing significantly increased tonic inhibition in peri-infarct cortex (asterisk, $P < 0.05$; see Supplementary Fig. 2 for further analyses). **c, d**, Representative traces showing tonic inhibitory currents in control and peri-infarct neurons, respectively. Tonic currents were revealed by the shift in holding currents after blocking all GABA$_A$ receptors with gabazine (>100 μM). Cells were voltage clamped at +10 mV.

[1]Department of Neurology, The David Geffen School of Medicine at UCLA, 635 Charles Young Drive South, Los Angeles, California 90095, USA. [2]Interdepartmental PhD Program for Neuroscience, The David Geffen School of Medicine at UCLA, 635 Charles Young Drive South, Los Angeles, California 90095, USA. [3]Department of Physiology, The David Geffen School of Medicine at UCLA, 635 Charles Young Drive South, Los Angeles, California 90095, USA. †Present address: Departments of Psychology and Anatomy and Structural Biology, University of Otago, PO Box 913, Dunedin 9013, New Zealand. *These authors contributed equally to this work.

(Supplementary Fig. 3a, c). The mean phasic inhibition was unchanged except for a transient decrease at 7 days after stroke (Supplementary Fig. 3b, d). The resting membrane and GABA reversal potentials were both unchanged (Supplementary Fig. 3e, f).

Tonic inhibition is effectively controlled by the degree of extracellular GABA uptake through neuronal and astrocytic GATs[14]. We applied a GAT-1-selective antagonist, NO-711 (10 μM), and found a significantly greater effect (percentage increase in I_{tonic} after GAT blockade) in post-stroke neurons (94.0 ± 16.3%, $n = 10$) than in controls (34.3 ± 11.4%, $n = 6$; $P < 0.05$; Fig. 2a). Co-application of NO-711 and the GAT-3/GAT-4-selective antagonist SNAP-5114 (40 μM) produced a substantial increase in I_{tonic} in controls (300.6 ± 46.0%, $n = 4$; Fig. 2a), revealing the synergistic actions of GATs in the cortex as previously proposed[17]. In post-stroke neurons, co-application only produced an effect (110.7 ± 32.0%, $n = 5$) similar to GAT-1 blockade alone ($P = 0.68$; Fig. 2a), indicating a dysfunction in GAT-3/GAT-4 after stroke. Sequential blockade of the two GATs confirmed the impairment after stroke, as peri-infarct I_{tonic} showed no further response to GAT-3/GAT-4 blockade after the initial GAT-1 block, in contrast to responses shown in controls (Fig. 2b, c). This effect was not due to receptor saturation, as I_{tonic} showed a further increase in response to a raised concentration of GABA under GAT blockade (Supplementary Fig. 4a). Western-blot analysis confirmed a reduced GAT-4 level in peri-infarct cortex, whereas GAT-1 levels were unchanged (Supplementary Fig. 5).

We proposed that the chronically raised tonic inhibition in the peri-infarct region may antagonize the neuronal plasticity required for functional recovery after stroke. Therefore, we tested whether reducing the excessive tonic inhibition would improve functional recovery. Of the two GABA$_A$ receptor subtypes shown to underlie tonic inhibition in cortical neurons, α5-GABA$_A$ receptors can be antagonized specifically by L655,708, a benzodiazepine inverse agonist[16], whereas no specific antagonist exists for δ-GABA$_A$ receptors. L655,708 (100 nM) decreased I_{tonic} in control neurons by −13.3 ± 5.2% ($n = 4$), but produced a significantly greater decrease in post-stroke neurons (−30.0 ± 4.1%, $n = 13$; $P < 0.05$; Fig. 2d, e), which reverted I_{tonic} back to control level (control: see earlier versus after stroke plus L655,708: 140.8 ± 18.5 pA, $n = 13$; $P = 0.702$; Fig. 2f). L655,708 produced only minimal effects on phasic inhibitory currents in both post-stroke and control conditions (Supplementary Fig. 4b).

Next we tested the effects of reducing tonic inhibition on functional recovery after stroke, using measures of forelimb and hindlimb motor control. Stroke produced an increase in the number of foot faults in the grid-walking task, and a decrease in forelimb symmetry in the cylinder task from 7 days after stroke. Chronic treatment with L655,708 starting 3 days after stroke resulted in a dose-dependent maximal gain of function beginning from 7 days after stroke in both tasks ($P < 0.001$; Fig. 3a–c). Acute treatment with L655,708 just before behavioural testing had a minimal effect on stroke recovery (Supplementary Fig. 7). To assess the necessity of long-term administration, we discontinued
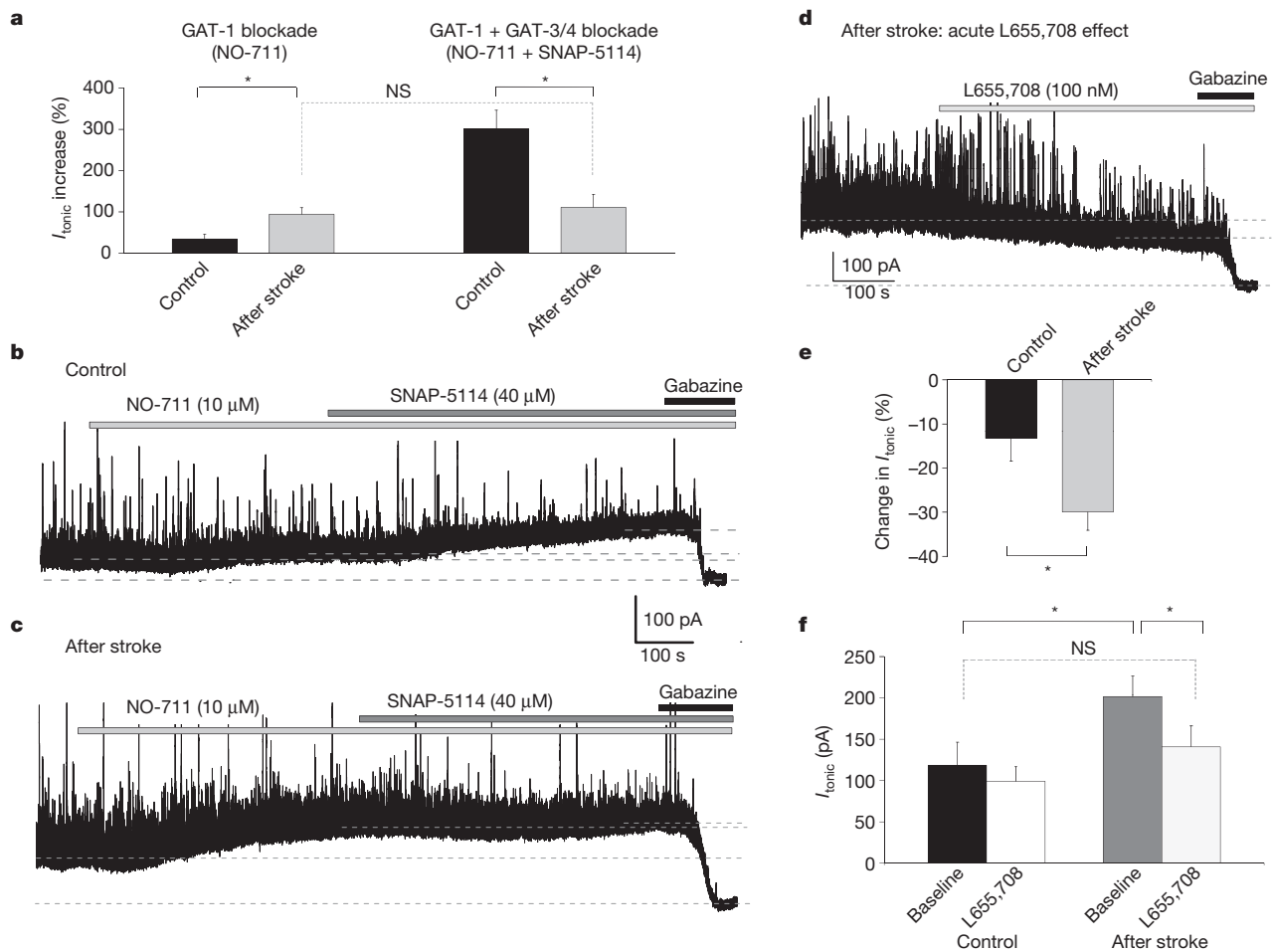

Figure 2 | Impairment in GABA transport and effect of blocking α5-GABA$_A$ receptors after stroke. a, Blocking GAT-1 (NO-711) produced a higher percentage increase in I_{tonic} after stroke; combined blockade of GAT-1 and GAT-3/GAT-4 (NO-711 plus SNAP-5114) produced a substantial I_{tonic} increase in controls but only an increase equivalent to blocking GAT-1 alone after stroke. **b, c**, I_{tonic} in sequential drug applications. Note the lack of response to SNAP-5114 application in the post-stroke slice. **d**, L655,708 reduced I_{tonic}. **e**, L655,708 significantly decreased I_{tonic} after stroke. **f**, Drug treatment reverted post-stroke I_{tonic} to near-control level. *, $P < 0.05$; NS, not significant; bar graphs represent mean ± s.e.m.

L655,708 treatment after 2 weeks and found a decrease in functional gains, although these mice still performed better than vehicle-treated stroke controls (Supplementary Fig. 6).

To corroborate further the role of reduced tonic inhibition in enhancing stroke recovery, we tested mice with deletions of either α5- or δ-subunit-containing GABA$_A$ receptors (Gabra5$^{-/-}$ and Gabrd$^{-/-}$; Methods)[18]. Gabra5$^{-/-}$ animals showed significantly better motor recovery after stroke, comparable to L655,708-treated wild-type animals (Fig. 3d–f). In addition, Gabra5$^{-/-}$ animals showed a significant reduction in hindlimb foot faults (Fig. 3e). Gabrd$^{-/-}$ animals also showed significant improvements in motor recovery (Fig. 3d–f), but to a lesser extent than the Gabra5$^{-/-}$ mice. Thus, modulation of α5-GABA$_A$ receptors affords greater functional gains in motor recovery than δ-GABA$_A$ receptors, and genetic removal of α5-GABA$_A$ receptors produces a more widespread increase in motor recovery than pharmacological antagonism. Administration of L655,708 to Gabrd$^{-/-}$ mice produced an even greater recovery, confirming the beneficial effect of reducing peri-infarct tonic inhibition (Fig. 3a, c).

Low/sub-seizure dosing of picrotoxin (PTX; 0.1 mg kg^{-1}, administered intraperitoneally (i.p.)), a use-dependent GABA$_A$ receptor antagonist, enhances learning and memory in transgenic mouse models of Alzheimer's and other cognitive impairments by reversing

an increased GABAergic inhibitory tone, acting at both synaptic and extrasynaptic GABA$_A$ receptors[19,20]. The pharmacological effects of PTX on reducing phasic and tonic inhibition were not altered after stroke (Supplementary Table 2). PTX given to animals from 3 days after stroke resulted in a significant gain of forelimb function on the grid-walking task compared to vehicle-treated stroke controls ($P < 0.05$; Supplementary Fig. 9a). No significant changes were observed in hindlimb function or forelimb asymmetry (Supplementary Fig. 9b, c). Combined L655,708 and PTX treatment showed similar initial functional gains compared to stroke and L655,708 alone; however, prolonged PTX and L655,708 treatment produced a deterioration in motor function such that the performance progressively worsened at late periods after stroke (Supplementary Fig. 9). These data indicate that increasing cortical excitability too far or reducing phasic inhibition negatively affects functional recovery.

An important element in stroke treatment is the timing of drug delivery. GABA$_A$ receptor agonists administered at the time of stroke decrease stroke size[20]. Therefore, dampening tonic inhibition too early after stroke may produce an opposite effect, that is, increased cell death. To test this, we assessed stroke volume at 7 days after stroke, in animals treated with 1) vehicle; 2) L655,708 from stroke onset; and 3) L655,708 from day 3 after stroke. Stroke volumes were similar between mice
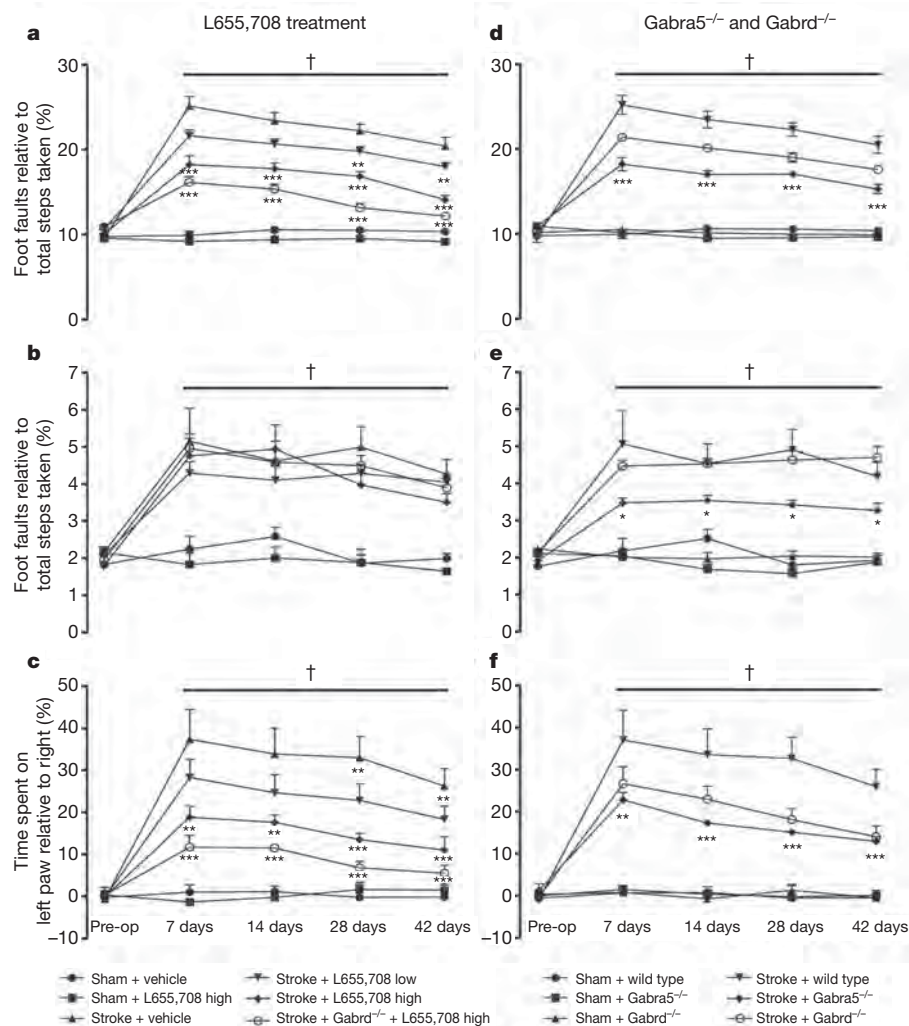

Figure 3 | Behavioural recovery after stroke with L655,708 treatment and in Gabra5$^{-/-}$ and Gabrd$^{-/-}$ animals. a–c, L655,708 treatment starting from 3 days after stroke resulted in a dose-dependent improvement in functional recovery after stroke. d–f, Gabra5$^{-/-}$ and Gabrd$^{-/-}$ mice also showed decreased motor deficits after stroke. Functional recovery was assessed with forelimb (a, d) and hindlimb foot faults (b, e), and on forelimb asymmetry (c, f). Low-dose L655,708 = 200 μg kg^{-1} day^{-1} per animal; high-dose L655,708 = 400 μg kg^{-1} day^{-1} per animal. Pre-op, pre-operation. Data are mean ± s.e.m. †, $P \leq 0.001$ stroke plus vehicle versus sham; *, $P \leq 0.05$; **, $P \leq 0.01$; ***, $P \leq 0.001$ versus stroke plus vehicle.
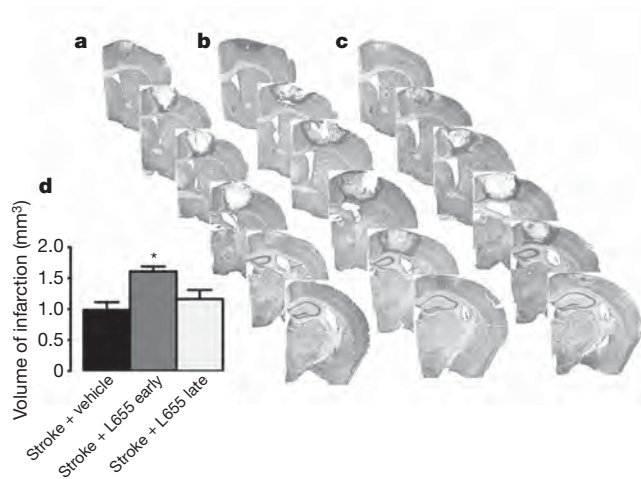
Figure 4 | Inflection point in L655,708 treatment effect on infarct size.
a–d, Representative Nissl-stained sections at 7 days after stroke from stroke
plus vehicle treatment (**a**), stroke plus L655,708 treatment starting at the time of
stroke (**b**) and stroke plus L655,708-treatment starting from 3 days post-insult
(**c**). Quantification of the stroke volume is shown in panel **d**. Data are
mean ± s.e.m. for $n = 4$ per group; * = $P \leq 0.05$.

METHODS SUMMARY

Photothrombotic model of focal stroke. Focal stroke was induced by photo-thrombosis in adult male C57BL/6 mice (aged 2–4 months) as described previously[27].
Slice preparation for electrophysiology. Following decapitation, brains were rapidly removed and placed into an *N*-methyl-D-glucamine (NMDG)-based cutting solution to enhance neuronal viability[28]. Coronal slices (350 μm) were cut and transferred to an interface-style chamber containing artificial cerebrospinal fluid (ACSF) as previously described[13]. Recordings were made from intact peri-infarct cortical layer-2/3 pyramidal neurons and analysed as previously described[13].
In vivo **drug administration.** L655,708 was dissolved in dimethylsulphoxide (DMSO) and then diluted 1:1 in 0.9% saline. L655,708-filled ALZET-1002 pumps were implanted at 3 days after stroke and replaced every two weeks. In acute administration studies, 5 mg kg^{-1} L655,708 was administered i.p. 30 min before testing. The concentration in one minipump, 5 mM, delivers a 200 μg kg^{-1} day^{-1} dose in mice. With one or two minipumps implanted, this provides a dose escalation. PTX (0.1 mg kg^{-1} i.p. twice a day) starting 3 days after stroke was administered alone or together with L655,708.
Behavioural analysis. Mice were videotaped during walking and exploratory behaviour in the grid-walking and cylinder/rearing tasks, and were tested at approximately the same time each day during the nocturnal period[29]. Baseline behavioural measurements were obtained one week before surgery. Post-stroke animals were assessed at weeks 1, 2, 4 and 6.
Infarct-size measurement. For the histological assessment of infarct size, brains were processed at 7 days after stroke using cresyl violet as previously described[30].
Statistical analyses. All data are expressed as mean ± s.e.m. For electrophysiological comparisons between control and post-stroke animals, the Mann–Whitney non-parametric test was used. For multiple comparisons across days after stroke, one-way analysis of variance (ANOVA) and Newman–Keuls' multiple pair-wise comparisons for post-hoc comparisons were used. For behavioural testing, differences between treatment groups were analysed using two-way ANOVA with repeated measures and Newman–Keuls' multiple pair-wise comparisons. The level of significance was set at $P < 0.05$.

Full Methods and any associated references are available in the online version of the paper at www.nature.com/nature.

treated with vehicle and L655,708 from day 3 (Fig. 4). In contrast, stroke volume was significantly increased in animals treated with L655,708 from stroke onset ($P < 0.05$; Fig. 4). These data indicate a critical timeframe for therapeutically dampening tonic inhibition after stroke: reduction too early would exacerbate stroke damage, whereas delaying treatment by 3 days would promote functional recovery without altering stroke size. Genetic deletion of α5- or δ-GABA$_A$ receptors did not affect infarct size or neuronal number in peri-infarct cortex (Supplementary Fig. 8). Unlike pharmacological antagonism of α5-GABA$_A$-receptor-mediated inhibition, in Gabra5$^{-/-}$ and Gabrd$^{-/-}$ mice, the genomic absence of one of the extrasynaptic GABA$_A$ receptors may trigger compensatory upregulation of the other receptor[13], thus obscuring their roles in neuroprotection immediately after stroke.

Current therapies that promote functional recovery after stroke are limited to physical rehabilitation[4]. Here, by identifying an excessive tonic inhibition after stroke, we have found promising new targets for pharmacological interventions to promote recovery. The increase in tonic inhibition in cortical pyramidal neurons occurs during precisely the same time period important for cortical map plasticity and recovery[1–3]. Alterations in other aspects of cortical signalling have also been described during this period, including altered GABA$_A$ receptor subunits, glutamate receptor expression and neuronal network properties[21–24]. Protein levels of GAT-1 were shown to be decreased in peri-infarct cortex in some rodent stroke models, and reactive astrocytes show reduced uptake of other neurotransmitters[24]. However, there are conflicting data on GABA$_A$ receptor levels after stroke[23–26]. We found a decreased protein level and compromised function of GAT-3/GAT-4 in peri-infarct cortex. The increase in tonic inhibition may curtail cortical plasticity and spontaneous recovery after stroke, and is consistent with tonic GABAergic inhibition exerting a causal role in limiting motor recovery in stroke.

Non-selectively decreasing GABAergic tone facilitates neuronal plasticity in genetic models of cognitive diseases[19,20]. We show for the first time, to our knowledge, that antagonizing a raised tonic inhibition enhances motor recovery after stroke, consistent with the idea that molecular and cellular events of neuronal plasticity are dampened in the peri-infarct zone, and promoting this plasticity facilitates functional recovery. Together, our results have identified novel pharmacological targets and provide a rational basis for developing future therapies to promote recovery after stroke and possibly other brain injuries.

1. Cramer, S. C. Repairing the human brain after stroke: I. Mechanisms of spontaneous recovery. *Ann. Neurol.* **63**, 272–287 (2008).
2. Brown, C. E., Aminoltejari, K., Erb, H., Winship, I. R. & Murphy, T. H. *In vivo* voltage-sensitive dye imaging in adult mice reveals that somatosensory maps lost to stroke are replaced over weeks by new structural and functional circuits with prolonged modes of activation within both the peri-infarct zone and distant sites. *J. Neurosci.* **29**, 1719–1734 (2009).
3. Dijkhuizen, R. M. *et al.* Correlation between brain reorganization, ischemic damage, and neurologic status after transient focal cerebral ischemia in rats: a functional magnetic resonance imaging study. *J. Neurosci.* **23**, 510–517 (2003).
4. Dobkin, B. H. Training and exercise to drive poststroke recovery. *Nature Clin. Pract. Neurol.* **4**, 76–85 (2008).
5. Carmichael, S. T. Cellular and molecular mechanisms of neural repair after stroke: making waves. *Ann. Neurol.* **59**, 735–742 (2006).
6. Nudo, R. J. Mechanisms for recovery of motor function following cortical damage. *Curr. Opin. Neurobiol.* **16**, 638–644 (2006).
7. Alonso-Alonso, M., Fregni, F. & Pascual-Leone, A. Brain stimulation in poststroke rehabilitation. *Cerebrovasc. Dis.* **24** (suppl. 1), 157–166 (2007).
8. Di Lazzaro, V. *et al.* Motor cortex plasticity predicts recovery in acute stroke. *Cereb. Cortex* **20**, 1523–1528 (2010).
9. Hensch, T. K. Critical period plasticity in local cortical circuits. *Nature Rev. Neurosci.* **6**, 877–888 (2005).
10. Donoghue, J. P., Suner, S. & Sanes, J. N. Dynamic organization of primary motor cortex output to target muscles in adult rats. II. Rapid reorganization following motor nerve lesions. *Exp. Brain Res.* **79**, 492–503 (1990).
11. Foeller, E., Celikel, T. & Feldman, D. E. Inhibitory sharpening of receptive fields contributes to whisker map plasticity in rat somatosensory cortex. *J. Neurophysiol.* **94**, 4387–4400 (2005).
12. Hess, G., Aizenman, C. D. & Donoghue, J. P. Conditions for the induction of long-term potentiation in layer II/III horizontal connections of the rat motor cortex. *J. Neurophysiol.* **75**, 1765–1778 (1996).
13. Glykys, J. & Mody, I. Hippocampal network hyperactivity after selective reduction of tonic inhibition in GABA$_A$ receptor α5 subunit-deficient mice. *J. Neurophysiol.* **95**, 2796–2807 (2006).
14. Walker, M. C. & Semyanov, A. Regulation of excitability by extrasynaptic GABA(A) receptors. *Results Probl. Cell Differ.* **44**, 29–48 (2008).
15. Collinson, N. *et al.* Enhanced learning and memory and altered GABAergic synaptic transmission in mice lacking the α5 subunit of the GABA$_A$ receptor. *J. Neurosci.* **22**, 5572–5580 (2002).

16. Atack, J. R. *et al.* L-655,708 enhances cognition in rats but is not proconvulsant at a dose selective for α5-containing GABA$_A$ receptors. *Neuropharmacology* **51,** 1023–1029 (2006).

17. Keros, S. & Hablitz, J. J. Subtype-specific GABA transporter antagonists synergistically modulate phasic and tonic GABA$_A$ conductances in rat neocortex. *J. Neurophysiol.* **94,** 2073–2085 (2005).

18. Glykys, J. & Mody, I. Activation of GABA$_A$ receptors: views from outside the synaptic cleft. *Neuron* **56,** 763–770 (2007).

19. Yoshiike, Y. *et al.* GABA$_A$ receptor-mediated acceleration of aging-associated memory decline in APP/PS1 mice and its pharmacological treatment by picrotoxin. *PLoS ONE* **3,** e3029 (2008).

20. Cui, Y. *et al.* Neurofibromin regulation of ERK signaling modulates GABA release and learning. *Cell* **135,** 549–560 (2008).

21. Ginsberg, M. D. Neuroprotection for ischemic stroke: past, present and future. *Neuropharmacology* **55,** 363–389 (2008).

22. Que, M. *et al.* Changes in GABA(A) and GABA(B) receptor binding following cortical photothrombosis: a quantitative receptor autoradiographic study. *Neurosci. Lett.* **93,** 1233–1240 (1999).

23. Redecker, C., Luhmann, H. J., Hagemann, G., Fritschy, J. M. & Witte, O. W. Differential downregulation of GABA$_A$ receptor subunits in widespread brain regions in the freeze-lesion model of focal cortical malformations. *J. Neurosci.* **20,** 5045–5053 (2000).

24. Frahm, C. *et al.* Regulation of GABA transporter mRNA and protein after photothrombotic infarct in rat brain. *J. Comp. Neurol.* **478,** 176–188 (2004).

25. Neumann-Haefelin, T. *et al.* Immunohistochemical evidence for dysregulation of the GABAergic system ipsilateral to photochemically induced cortical infarcts in rats. *Neuroscience* **87,** 871–879 (1998).

26. Kharlamov, E. A., Downey, K. L., Jukkola, P. I., Grayson, D. R. & Kelly, K. M. Expression of GABA$_A$ receptor α1 subunit mRNA and protein in rat neocortex following photothrombotic infarction. *Brain Res.* **1210,** 29–38 (2008).

27. Lee, J. K., Kim, J. E., Sivula, M. & Strittmatter, S. M. Nogo receptor antagonism promotes stroke recovery by enhancing axonal plasticity. *J. Neurosci.* **24,** 6209–6217 (2004).

28. Tanaka, Y., Furuta, T., Yanagawa, Y. & Kaneko, T. The effects of cutting solutions on the viability of GABAergic interneurons in cerebral cortical slices of adult mice. *J. Neurosci. Methods* **171,** 118–125 (2008).

29. Baskin, Y. K., Dietrich, W. D. & Green, E. J. Two effective behavioral tasks for evaluating sensorimotor dysfunction following traumatic brain injury in mice. *J. Neurosci. Methods* **129,** 87–93 (2003).

30. Ohab, J. J., Fleming, S., Blesch, A. & Carmichael, S. T. A neurovascular niche for neurogenesis after stroke. *J. Neurosci.* **26,** 13007–13016 (2006).

Author Contributions A.N.C. performed the behavioural, histological and immunohistochemical studies; B.S.H. carried out the electrophysiological experiments; and S.E.M. performed the immunohistochemical and western blot work. A.N.C., B.S.H., I.M. and S.T.C. designed the experiments, analysed data, prepared figures and wrote the manuscript.

Author Information Reprints and permissions information is available at www.nature.com/reprints. The authors declare no competing financial interests. Readers are welcome to comment on the online version of this article at www.nature.com/nature. Correspondence and requests for materials should be addressed to S.T.C. (scarmichael@mednet.ucla.edu).

METHODS

Photothrombotic model of focal stroke. Under isoflurane anaesthesia (2–2.5% in a 70% N_2O/30% O_2 mixture), 2–4 month-old adult C57BL/6 (Charles River) male mice were placed in a stereotactic apparatus, the skull exposed through a midline incision, cleared of connective tissue and dried. A cold light source (KL1500 LCD, Zeiss) attached to a 40× objective giving a 2-mm diameter illumination was positioned 1.5 mm lateral from Bregma, and 0.2 ml of Rose Bengal solution (Sigma; $10 \, g \, l^{-1}$ in normal saline, i.p.) was administered[31]. After 5 min, the brain was illuminated through the intact skull for 15 min. Rose Bengal produces singlet oxygen under light excitation, which damages and occludes vascular endothelium, resulting in focal cortical stroke under the region of illumination (Fig. 4), circumscribed by peri-infarct tissue with normal neuronal cell number (Supplementary Fig. 8). Two-to-four-month-old adult male $Gabra5^{-/-}$ and $Gabrd^{-/-}$ mice[32] received a stroke as described earlier. These mice had been backcrossed to C57BL/6 mice in excess of 15 generations, and were compared in behavioural studies to wild-type C57BL/6. Body temperature was maintained at $36.9 \pm 0.4 \, ^\circ C$ with a heating pad throughout the operation and did not vary by drug or genetic condition. This stroke method produces a small stroke in the mouse forelimb region of the motor cortex (Fig. 4). Sample size was ten per group for $Gabra5^{-/-}$ and $Gabrd^{-/-}$ in stroke/behavioural studies. Sample size was eight per group for each condition in dosing of L655,708 (Fig. 3).

Blood pressure (systolic and diastolic) and heart rate were measured in separate cohorts of wild-type (C57BL/6) mice, with or without L655,708 administration via ALZET minipumps from 3 days after stroke, and in $Gabra5^{-/-}$ and $Gabrd^{-/-}$ mice, before, during and after stroke, using a standard non-invasive tail-cuff method (Coda). There were no significant differences in heart rate or blood pressure by treatment or genotype (Supplementary Table 1). All studies in this manuscript complied with the Stroke Therapy Academic Industry Roundtable (STAIR) criteria[33,34] for stroke investigations in measuring physiological parameters, monitoring treatment effects for at least one month, analysing treatment effects blinded to conditions, using dose–response studies and use of a drug administration route with blood–brain-barrier penetration.

Whole-cell voltage-clamp electrophysiology. Slices were submerged in the recording chamber and continuously perfused ($5–8 \, ml \, min^{-1}$) with oxygenated ACSF ($32–34 \, ^\circ C$). Visualized patch-clamp recordings from layer-2/3 pyramidal neurons were performed at 40× using infrared oblique-illumination (Leica DM-LFS; Hamamatsu CCD camera C3077-78).

Control recordings were made from cells of sham-operated animals at similar locations as those recorded in post-stroke animals. Microelectrodes ($3–5 \, M\Omega$) were filled with a cesium-methylsulphonate ($CsMeSO_4$)-based internal pipette solution, containing 120 mM $CsMeSO_4$, 10 mM CsCl, 5 mM TEA-Cl, 1.5 mM $MgCl_2$, 10 mM HEPES, 0.1 mM EGTA, 2 mM Na-ATP, 0.5 mM Na-GTP and 5 mM QX-314, pH 7.25–7.30 with CsOH, 275–285 mOsm. The recording ACSF was supplemented with 5 μM GABA to replenish the extracellular GABA concentration reduced by the high-flow perfusion of the slices[32]. For recording I_{tonic} at $-70 \, mV$, a high-CsCl-based internal solution was used, containing 140 mM CsCl, 1 mM $MgCl_2$, 10 mM HEPES, 0.1 mM EGTA, 4 mM NaCl, 2 mM Mg-ATP, 0.3 mM Na-GTP and 5 mM QX-314, pH ~7.3, ~275 mOsm l^{-1}, with ACSF containing 3 mM kynurenic acid to block glutamatergic currents.

Neurons were voltage clamped in whole-cell configuration using a MultiClamp-700A amplifier (Molecular Devices); all recordings were low-pass-filtered at 3 kHz (8-pole Bessel) and digitized online at 10 kHz (National Instruments PCI-MIO-16E-4 board). Series resistance and whole-cell capacitance were estimated from fast transients evoked by a 5-mV step and compensated to 75%. Excitatory postsynaptic currents (EPSCs) and inhibitory postsynaptic currents (IPSCs) were recorded by voltage clamping sequentially at $-70 \, mV$ and $+10 \, mV$, respectively.

All drugs were purchased from Sigma or Tocris. L-655,708 and SNAP-5114 were dissolved in DMSO then diluted 1:1,000 in H_2O. NO-711, gabazine and GABA were dissolved in H_2O.

Tonic inhibitory current and mean phasic current determination. Custom-written macros running under IGOR Pro v.6.0 (WaveMetrics) were used to analyse the digitized recordings to determine the values of tonic currents and mean phasic currents, as previously described[31]. I_{tonic} was recorded as the reduction in baseline holding currents (I_{hold}) after bath-applying a saturating amount (>100 μM) of the $GABA_A$-receptor antagonist SR-95531 (gabazine), while voltage clamping at $+10 \, mV$. NO-711, SNAP-5114 and L-655,708 were added to the recording ACSF via perfusion and their effects on I_{tonic} were recorded as the post-drug shift in I_{hold}. Drug perfusion was continued until the shifting I_{hold} remained steady for 1–2 min.

To determine the mean phasic current (I_{mean}), a 60-s segment containing either EPSCs or IPSCs was selected, and an all-point histogram was plotted for every 10,000 points (every 1 s), smoothed, and fitted with a Gaussian to obtain the mean baseline current. All baseline mean values were then plotted and linear trends subtracted to normalize the mean baseline current to 0 pA. After baseline normalization, the values of each 10,000 points (each 1 s) were averaged to yield the value of I_{mean} (in $pA \, s^{-1}$) for each 1-s epoch. The averaged I_{mean} value of a 60-s segment was reported as the phasic I_{mean} value for either the spontaneous EPSC or IPSC. Synaptic event kinetics (that is, frequency, peak amplitude, 10–90% rise time and weighted decay time constant) are analysed by custom-written LabView-based software (EVAN), as previously described[32]. For comparison of the IPSC peak amplitudes under control and PTX-treated conditions (Supplementary Table 2), the largest-amplitude count-matched method[32] was used, whereby the amplitude values in a given recording were sorted and the largest x number of events under control conditions were averaged and compared to the average of an equally matched x number of events recorded during a similar time period under the PTX condition, with x being the total number of events detected under the 10 μM PTX condition. This method circumvents the erroneous comparison of average amplitudes when considering the effects of a receptor antagonist that reduces the smaller events (in control conditions) down to the noise level.

Measurements of neuronal resting membrane potential and GABA reversal potential. To estimate neuronal resting membrane potential (V_{rest}), the cell-attached recording technique[35,36] was used. Briefly, depolarizing voltage ramps (-100 to $+200 \, mV$) were applied to cell-attached patches to activate voltage-gated K^+ channels and establish the K^+ current reversal potential, which provides a measure of the V_{rest}, given near equimolar K^+ inside the cell and the pipette. The GABA reversal potential (E_{GABA}) was estimated by measuring the K^+ reversal potential after activating $GABA_A$ receptors with 50 μM muscimol. Recordings were made using a solution containing the following: 135 mM K^+ gluconate, 5 mM KCl, 2 mM $MgCl_2$, 10 mM HEPES, 0.1 mM EGTA, 4 mM Na-ATP, 0.3 mM Na-GTP, pH 7.3, 273 mOsm l^{-1}. A junction potential of 9 mV was measured and then subtracted from voltage values of all measurements.

Fitting of multiple distributions to cumulative probability plots. The fitting of multiple distributions to a cumulative probability plot (Supplementary Fig. 2) was done as follows. Cumulative probabilities of the variable x (that is, $P(x)$) were calculated and fitted by one or more normal curves approximated by the logistic equation[37]:

$$P(x) = \sum_{i=1}^{n} R_i \frac{x^{p_i}}{x^{p_i} + \bar{x}_i^{p_i}}$$

where $R_1 \ldots R_n$ are the ratios of the n normal distributions (such as $\sum_{i=1}^{n} R_n = 1$), $\bar{x}_1 \ldots \bar{x}_n$ are the individual means, and $p_1 \ldots p_n$ are steepness factors related to the n standard deviations ($s.d._1 \ldots s.d._n$).

Grid-walking task. The grid-walking apparatus was manufactured as previously described[38,39], using a 12-mm square wire mesh with a grid area of 32 cm/20 cm/50 cm (length/width/height). A mirror was placed beneath the apparatus to allow video footage in order to assess the animals' stepping errors (foot faults). Each mouse was placed individually on top of the elevated wire grid and allowed to freely walk for a period of 5 min. Video footage was analysed offline by raters blind to the treatment groups. The total number of foot faults for each limb, along with the total number of non-foot-fault steps, was counted, and a ratio between foot faults and total steps taken calculated. Per cent foot faults were calculated by: number of foot faults / (foot faults + number of non-foot-fault steps) × 100. A ratio between foot faults and total steps taken was used to take into account differences in the degree of locomotion between animals and trials. A step was considered a foot fault if it was not providing support and the foot went through the grid hole. Furthermore, if an animal was resting with the grid at the level of the wrist, this was also considered a fault. If the grid was anywhere forward of the wrist area then this was considered as a normal step.

Spontaneous forelimb task (cylinder task). The spontaneous forelimb task encourages the use of forelimbs for vertical wall exploration/press in a cylinder[38,39]. When placed in a cylinder, the animal rears to a standing position, while supporting its weight with either one or both of its forelimbs on the side of the cylinder wall. Mice were placed inside a Plexiglas cylinder (15 cm in height with a diameter of 10 cm) and videotaped for 5 min. Videotaped footage of animals in the cylinder was evaluated quantitatively in order to determine forelimb preference during vertical exploratory movements. While the video footage was played in slow motion (1/5th real time speed), the time (seconds) during each that each animal spent on either the right forelimb, the left forelimb, or on both forelimbs were calculated. Only rears in which both forelimbs could be clearly seen were timed. The percentage of time spent on each limb was calculated and these data were used to derive an SFL asymmetry index ((per cent ipsilateral use) − (per cent contralateral use)). The 'contact time' method of examining the behaviour was chosen over the 'contact placement' method, as described in ref. 38, as it takes into account the slips that often occur during a bilateral wall press after photothrombosis.

Western blot. Seven days after stroke mice were decapitated, the brains rapidly removed and peri-infarct cortex microdissected and frozen ($n = 5$). The equivalent region of cortex was taken in control, non-operated mice ($n = 3$). Samples were homogenized in radioimmunoprecipitation (RIPA) buffer (Pierce) and centrifuged at 20,000g at $4 \, ^\circ C$ for 10 min. Supernatant was collected as protein extract

and stored at −80 °C. Western blot was performed as described[40]. One-hundred micrograms of protein from each sample was diluted in 7.5 μl of 2× SDS-sample buffer gel (Invitrogen) containing dithiothreitol (DTT) (Sigma) and brought to a final volume of 15 μl with RIPA buffer. Samples were denatured at 95 °C, loaded on to a 4–12% gradient Tris-Glycine gel (Invitrogen), separated via SDS–polyacrylamide gel electrophoresis (PAGE), and then transferred to HYBOND-P (PVDF) membrane (Amersham) at 30 V for 2 h. Membranes were rinsed and blocked overnight at 4 °C. Membranes were probed with antibodies against GABA transporter 3 (rabbit anti-GAT-3 1:1,000; Millipore), and GABA transporter 1 (rabbit anti-GAT-1 1:200; Millipore). Following successive washes, membranes were incubated in IgG donkey anti-rabbit horseradish peroxidise (HRP)-labelled secondary (1:6,000; Jackson) for 1 h at room temperature (21–23 °C). Membranes were incubated in ECL PLUS (Amersham) and chemiluminescence was detected using Fluorochem (Alpha Innotech). Membranes were then re-probed for 1 h at room temperature (21–23 °C) with GAPDH (1:2,500; Abcam) and donkey anti-rabbit-HRP (1:10,000; Jackson) as an endogenous control protein to ensure equal loading. Immunoblotting was performed in triplicate for each antibody. Adobe Photoshop software (Adobe Systems) was used for densitometric analysis of all blots.

31. Lee, K., Kim, J. E., Sivula, M. & Strittmater, S. M. Nogo receptor antagonism promotes stroke recovery by enhamcing axonal plasticity. *J. Neurosci.* **24,** 6209–6217 (2004).

32. Glykys, J., Mann, E. O. & Mody, I. Which GABA$_A$ receptor subunits are necessary for tonic inhibition in the hippocampus? *J. Neurosci.* **28,** 1421–1426 (2008).

33. STAIR. Recommendations for standards regarding preclinical neuroprotective and restorative drug development. *Stroke.* **30,** 2752–2758 (1999).

34. Fisher, M., Feuerstein, G., Howells, D. W., Hurn, P. D., Kent, T. A., Savitz, S. I. & Lo, E. H. Update of the stroke therapy academic industry roundtable preclinical recommendations. *Stroke.* **40,** 2244–2250 (2009).

35. Stell, B. & Mody, I. Receptors with different affinities mediate phasic and tonic GABA$_A$ conductances in hippocampal neurons. *J. Neurosci.* **22,** RC223 (2002).

36. Verheugen, J. A., Fricker, D. & Miles, R. Noninvasive measurements of the membrane potential and GABAergic action in hippocampal interneurons. *J. Neurosci.* **19,** 2546–2555 (1999).

37. Barlow, R. Cumulative frequency curves in population analysis. *Trends Pharmacol. Sci.* **11,** 404–406 (1990).

38. Baskin, Y. K., Dietrich, W. D. & Green, E. J. Two effective behavioral tasks for evaluating sensorimotor dysfunction following traumatic brain injury in mice. *J. Neurosci. Methods* **129,** 87–93 (2003).

39. Schallert, T., Fleming, S. M., Leasure, J. L., Tillerson, J. L. & Bland, S. T. CNS plasticity and assessment of forelimb sensorimotor outcome in unilateral rat models of stroke, cortical ablation, parkinsonism and spinal cord injury. *Neuropharmacology* **39,** 777–787 (2000).

40. Moore, C. S. *et al.* Increased X-linked inhibitor of apoptosis protein (XIAP) expression exacerbates experimental autoimmune encephalomyelitis (EAE). *J. Neuroimmunol.* **203,** 79–93 (2008).